

A Journal of the Gesellschaft Deutscher Chemiker

# Angewandte Chemie

GDCh

International Edition

www.angewandte.org

## Accepted Article

**Title:** Thiazolo[5,4-d]thiazole-Based Donor-Acceptor Covalent Organic Frameworks for Sunlight-Driven Hydrogen Evolution

**Authors:** Wenqian Li, Xiaofeng Huang, Tengwu Zeng, Yahu A. Liu, Weibo Hu, Hui Yang, Yue-Biao Zhang, and Ke Wen

This manuscript has been accepted after peer review and appears as an Accepted Article online prior to editing, proofing, and formal publication of the final Version of Record (VoR). This work is currently citable by using the Digital Object Identifier (DOI) given below. The VoR will be published online in Early View as soon as possible and may be different to this Accepted Article as a result of editing. Readers should obtain the VoR from the journal website shown below when it is published to ensure accuracy of information. The authors are responsible for the content of this Accepted Article.

**To be cited as:** *Angew. Chem. Int. Ed.* 10.1002/anie.202014408

**Link to VoR:** <https://doi.org/10.1002/anie.202014408>

## RESEARCH ARTICLE

# Thiazolo[5,4-*d*]thiazole-Based Donor-Acceptor Covalent Organic Frameworks for Sunlight-Driven Hydrogen Evolution

Wenqian Li,<sup>[a,c],#</sup> Xiaofeng Huang,<sup>[b],#</sup> Tengwu Zeng,<sup>[b]</sup> Yahu A. Liu,<sup>[d]</sup> Weibo Hu,<sup>[a]</sup> Hui Yang,<sup>\*,[a,b]</sup> Yue-Biao Zhang,<sup>\*,[b]</sup> and Ke Wen<sup>\*,[a,b]</sup>

[a] W. Q. Li, W. B. Hu, Prof. H. Yang, Prof. K. Wen,  
Shanghai Advanced Research Institute  
Chinese Academy of Sciences  
Shanghai 201210, China  
E-mail: yangh@sari.ac.cn (H. Yang), wenk@sari.ac.cn (W. Ke)

[b] X. F. Huang, T. W. Zeng, Prof. Y. -B. Zhang  
School of Physical Science and Technology  
ShanghaiTech University  
Shanghai 201210, China

[c] W. Q. Li  
University of Chinese Academy of Sciences  
Beijing 100049, China

[d] Y. A. Liu  
Medicinal Chemistry  
ChemBridge Research Laboratories  
San Diego, CA 92127, USA

# These authors have contributed equally.

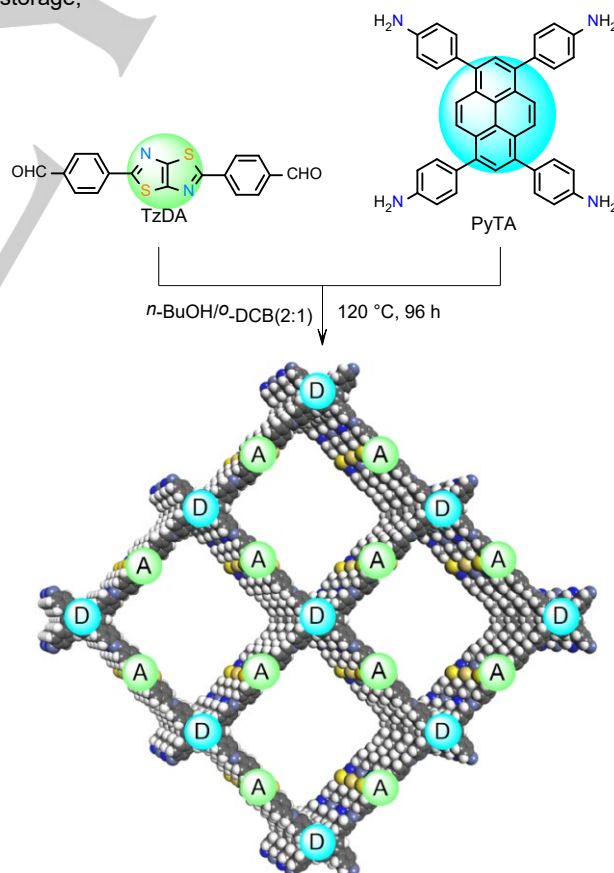
Supporting information for this article is given via a link at the end of the document.

**Abstract:** 2D covalent organic frameworks (COFs) could have well-defined arrangements of photo- and electro-active units that serve as electron or hole transport channels for solar energy harvesting and conversion, but their insufficient charge transfer and rapid charge recombination impede the sunlight-driven photocatalytic performance. We report a new donor-acceptor (D-A) system, PyTz-COF that was constructed from the electron-rich pyrene (Py) and electron-deficient thiazolo[5,4-*d*]thiazole (Tz). With its bicontinuous heterojunction, PyTz-COF demonstrated exceptional optoelectronic properties, photocatalytic ability in superoxide anion radical-mediated coupling of (arylmethyl)amines and photoelectrochemical activity in sunlight-driven hydrogen evolution. Remarkably, PyTz-COF exhibited a photocurrent up to 100  $\mu\text{A cm}^{-2}$  at 0.2 V vs. RHE and could reach a hydrogen evolution rate of 2072.4  $\mu\text{mol g}^{-1} \text{h}^{-1}$ . This work is paving the way for reticular design of highly efficient and highly active D-A systems for solar energy harvesting and conversion.

## Introduction

Since the introduction of the first useful water photolysis to generate hydrogen,<sup>[1]</sup> sunlight-driven photocatalytic hydrogen production has been considered as one of the most important renewable energy sources. Efforts have been made from the perspective of band-engineering,<sup>[2]</sup> surface morphology tuning<sup>[3]</sup> and defect modulation<sup>[4]</sup> to facilitate kinetics of photogenerated carriers. Reticular chemistry has offered a handle for systematic modulation of light absorption, band position, and photogenerated carriers at the molecular level.<sup>[5]</sup> Covalent organic frameworks (COFs) are materials by using reticular chemistry - linking organic building units through strong covalent bonds into extended 2D and 3D networks,<sup>[6]</sup> owing to their excellent thermal/chemical stabilities, permanent porosity, and electrochemical activity,

COFs have demonstrated great application potential in gas storage,



**Scheme 1.** Synthetic route of PyTz-COF under solvothermal conditions.

## RESEARCH ARTICLE

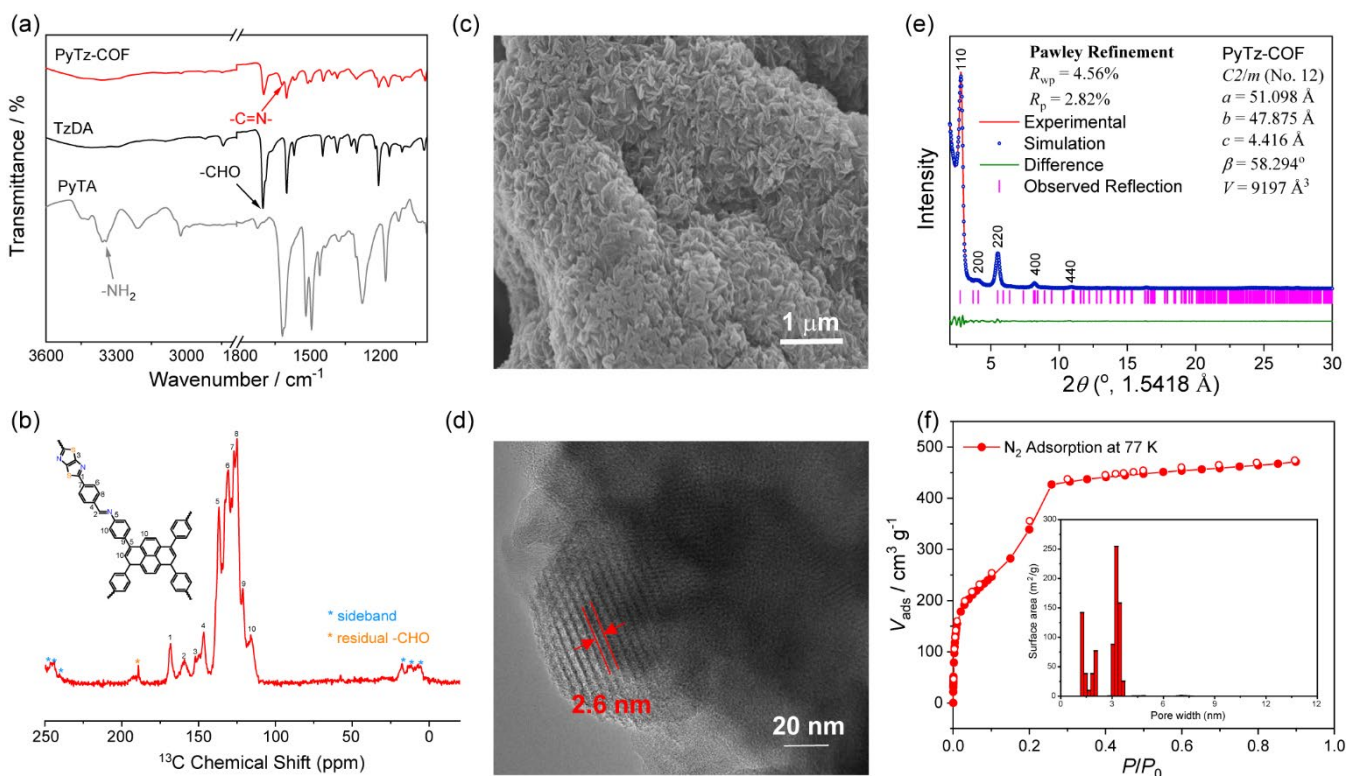


**Figure 1.** (a) FT-IR spectra of PyTz-COF, TzDA and PyTA. (b) Solid-state  $^{13}\text{C}$  CP-MAS NMR spectrum of PyTz-COF (spinning sidebands denoted by asterisks). (c) SEM image of PyTz-COF. (d) TEM image of PyTz-COF showing the lattice fringe perpendicular to the 1D channels (distance 2.6 nm). (e) PXRD patterns: experimental (red), simulated with eclipsed AA stacking mode (blue), difference (green) and the observed reflection (violet). (f)  $\text{N}_2$  sorption isotherms of activated PyTz-COF at 77 K and the derived pore size distribution.

adsorptive separation, flexible display, chemical sensing, energy conversion and storage, and chemical catalysis.<sup>[7]</sup> In particular, interconnection of electron-deficient and electron-rich building units in 2D donor-acceptor (D-A) COFs opened a new way for highly effective charge separation and charge transport.<sup>[8]</sup>

As an electron-deficient  $\pi$  building unit, thiazolo[5,4-*d*]thiazole (Tz) represents co-facial geometry and strong intermolecular  $\pi$ - $\pi$  stacking have been widely studied in dye molecules and conjugated polymers for photovoltaic, two-photon adsorption, non-linear optics, and photocatalytic applications.<sup>[9]</sup> Recently, Lotsch and co-workers have reported a Tz-based COF catalyst (TpTz COF) that exhibited excellent photo-absorbing ability in hydrogen evolution via solar water-splitting.<sup>[10]</sup> We conjectured that TpTz's photo-absorbing ability could be boosted if its 2,4,6-trivinylcyclohexane-1,3,5-trione (Tp) subunits were replaced by more electron-rich polycyclic  $\pi$  systems. 1,3,6,8-tetraphenylpyrene (Py) serves as a good chromophore as it extends the light absorption range compared to triazine unit adopted in covalent triazine frameworks (CTF).<sup>[11]</sup> Owing to its molecular size, strong electron donating property, and the interlayer ordered stacking,<sup>[12]</sup> the overlapping of  $\pi$ -orbitals of Py and Tz subunits with enhanced electron push-pull interaction would render a more efficient charge separation in formed 2D COF. Here, we report the design of a photoactive 2D COF from donor Py and acceptor Tz building units, which has shown remarkable photocatalytic activities<sup>[13]</sup> in superoxide anion-

mediated coupling of arylmethyl amines and Pt co-catalyzed sustained  $\text{H}_2$  evolution.<sup>[14]</sup>

## Results and Discussion

**Synthesis and Characterization.** PyTz-COF was synthesized via an imine condensation of 4,4',4'',4'''-(pyrene-1,3,6,8-tetrayl)tetraaniline (PyTA) and 4,4'-(thiazolo[5,4-*d*]thiazole-2,5-diyl)dibenzaldehyde (TzDA) in the presence of acetic acid in a mixed solvent of *n*-butyl alcohol (*n*-BuOH) and *o*-dichlorobenzene (*o*-DCB) (Scheme 1, Figure S1-S5, Supporting Information). The as-synthesized PyTz-COF was analyzed by Fourier-transform infrared (FT-IR) spectroscopy (Figure 1a), showing characteristic signal of  $\text{-C=N-}$  stretching at  $\sim 1620 \text{ cm}^{-1}$ , along with the disappearance of aniline N-H stretching bands between 3200 and 3400  $\text{cm}^{-1}$ . The signal at  $\sim 1696 \text{ cm}^{-1}$  ( $\text{C=O}$ ) could be attributed to terminal residual group of PyTz-COF. In solid-state  $^{13}\text{C}$  cross-polarization with magic-angle spinning (CP-MAS) NMR spectrum (Figure 1b), the signals located at 168 and 155 ppm could be attributed to carbon atoms of the Tz ring, and the ones from 120 to 150 ppm should belong to the Py carbons. All these data support the conversion of starting materials into an imine-linked structure.

The scanning electron microscopy (SEM) image revealed a petal-like morphology of PyTz-COF (Figure 1c). The transmission

## RESEARCH ARTICLE

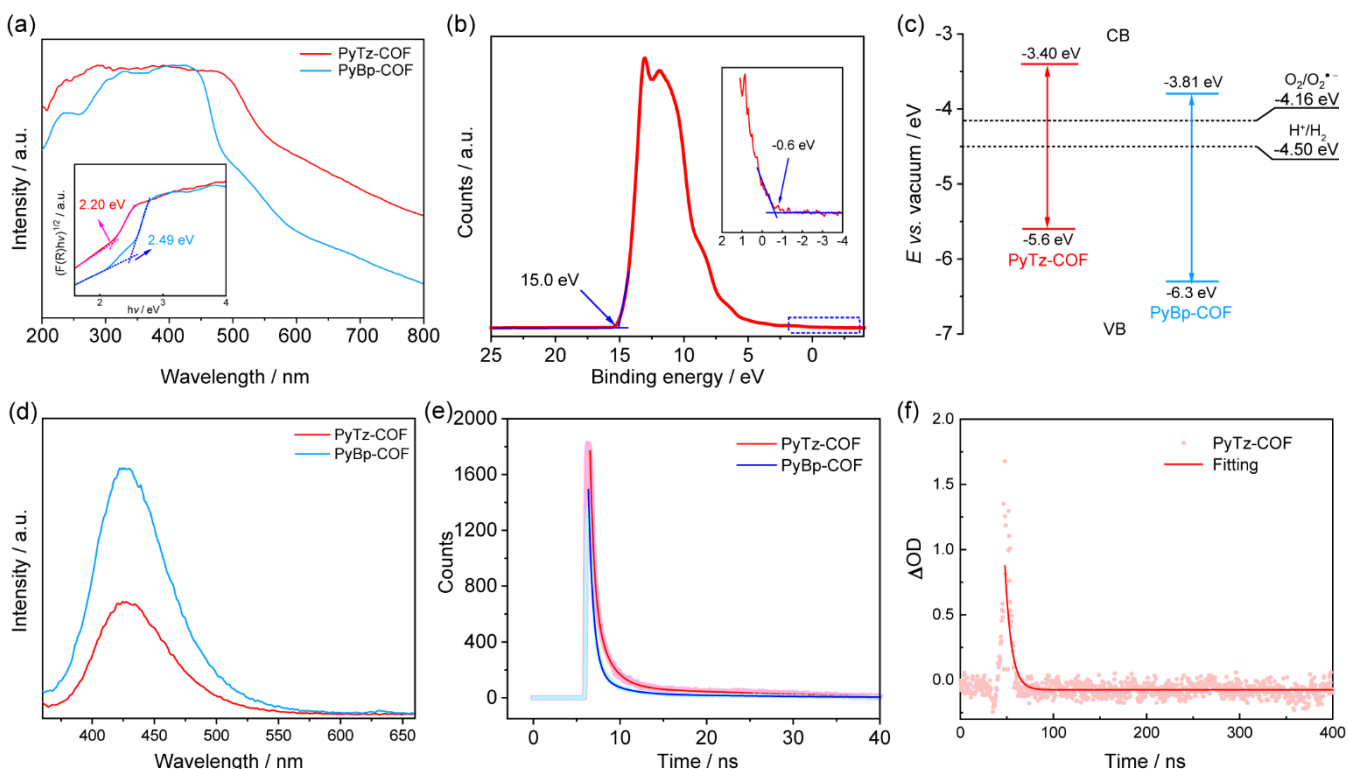


**Figure 2.** (a) UV/vis diffuse reflectance spectra of PyTz-COF and PyBp-COF. Inset: Band gaps determined by the Kubelka-Munk-transformed reflectance spectra (b) High-resolution valence band ultraviolet photoelectron spectra (UPS) of PyTz-COF. (c) Band structures of PyTz-COF and PyBp-COF and their thermodynamic equilibrium redox potentials for  $O_2$  and proton reduction in vacuum scale. (d) Photoluminescence spectra of PyTz-COF and PyBp-COF (excitation at 320 nm). (e) Time-resolved photoluminescence spectra of PyTz-COF and PyBp-COF (excitation at 320 nm). (f) Transient absorption spectrum of PyTz-COF's hole polarons (at 700 nm).

electron microscopy (TEM) image further brought to light 2D ordered arrays (Figure 1d). The high crystallinity of as-synthesized PyTz-COF was further confirmed by powder X-ray diffraction (PXRD) analysis, which showed the intense peaks of 110, 200, 220, 400, and 440 reflections. The experimental PXRD pattern was in good agreement with a sliding model that was derived from the eclipsed (AA) stacking mode. Pawley refinement provided lattice parameters with the space group of  $C2/m$  ( $a = 51.098 \text{ \AA}$ ,  $b = 47.875 \text{ \AA}$  and  $c = 4.416 \text{ \AA}$ ,  $\alpha = \gamma = 90^\circ$ ,  $\beta = 58.294^\circ$ ).

The permanent porosity of PyTz-COF was assessed by nitrogen adsorption isotherm measured at 77 K. The adsorption curves bear characteristic features of type IV isotherms (Figure 1f) with the Brunauer–Emmett–Teller (BET) surface area of  $1175 \text{ m}^2 \text{ g}^{-1}$ . Non-local density functional theory (NL-DFT) calculation discovered the pore size distribution centered at  $\sim 3.2 \text{ nm}$ , matching the predicted values ( $3.5 \text{ nm}$ ) of AA eclipsed framework geometry. The total pore volume of PyTz-COF at  $PIP_0 = 0.99$  was calculated to be  $0.77 \text{ cm}^3 \text{ g}^{-1}$ . These data provided enough evidence of the formation of mesoporous 2D COFs.

**Thermal and Chemical Stabilities.** In thermogravimetric analysis (TGA), PyTz-COF was found to be thermally stable up to  $400^\circ \text{C}$ , and more than 60% of its initial weight remained until  $750^\circ \text{C}$  (Figure S6, Supporting Information). The chemical stability of PyTz-COF was evaluated by soaking the COF sample in both protic and aprotic solvents [methanol (MeOH), tetrahydrofuran (THF), dimethyl sulfoxide (DMSO), and *N,N*-dimethylformamide (DMF)]. Neglectable changes in the intensities of characteristic peaks in PXRD patterns (Figure S7, Supporting Information) before and after 3-day soaking suggested PyTz-COF is

chemically stable in these solvents. Notably, PyTz-COF was stable even in harsh basic and acidic environments (in 3.0 M aqueous KOH and HCl solutions, respectively) for 3 days at least (Figure S7, Supporting Information). The decent chemical tolerance of PyTz-COF could be attributed to the planarity of the Tz and Py units and the overlapping of their  $\pi$  orbitals, which would allow strong  $\pi$ - $\pi$  interactions between the layers.

**Photoelectric Properties.** For comparison of photoelectric properties of donor-acceptor (D-A) and a non-D-A system, PyBp-COF<sup>[11a]</sup> constructed from PyTA and [1,1'-biphenyl]-4,4'-dicarbaldehyde (BpDA) was prepared (Supporting Information) and characterized (Figure S8–S11, Supporting Information). Both PyTz-COF (D-A) and PyBp-COF (non-DA) were studied using ultraviolet/visible diffuse reflectance spectroscopy (UV/vis DRS), ultraviolet photoelectron spectroscopy (UPS), photoluminescence (PL) spectroscopy and transient absorption spectroscopy (TAS).

In UV/vis DRS analysis (Figure 2a), while PyBp-COF showed the strongest absorption band at 480 nm, PyTz-COF exhibited an obvious red-shift with the strongest absorption band at 540 nm. Their optical band gaps were calculated as 2.49 eV and 2.20 eV for PyBp-COF and PyTz-COF, respectively (Figure 2a). Faster intramolecular charge transfer from the donor to acceptor and more extended  $\pi$ -electron delocalization in PyTz-COF enables wider range of light to be absorbed.<sup>[8a,15]</sup> On the basis of their UPS spectra (Figure 2b and Figure S12, Supporting Information), the relative valence band maximum (VBM) of PyBp-COF and PyTz-COF were calculated to be  $-6.3 \text{ eV}$  and  $-5.6 \text{ eV}$ , respectively. Thereby, the energies of conduction band minimum (CBM) of

## RESEARCH ARTICLE

PyBp-COF and PyTz-COF were determined to be  $-3.81$  eV and  $-3.40$  eV, respectively. Since the  $E_{\text{CB}}$  of PyTz-COF is greater than the potential of  $\text{O}_2/\text{O}_2^{\cdot-}$  ( $-4.16$  eV) or  $\text{H}^+/\text{H}_2$  ( $-4.50$  eV) (Figure 2c), PyTz-COF is anticipated to be able to reduce  $\text{O}_2$  to  $\text{O}_2^{\cdot-}$  or  $\text{H}^+$  to  $\text{H}_2$  upon photoexcitation.<sup>[16]</sup>

Photoluminescence (PL) spectroscopy was used to assess the ability of charge transfer and separation in the two COFs. At the same emission maxima of 425 nm, PyTz-COF exhibited a much weaker photoluminescence than that of PyBp-COF (Figure 2d), indicating that the radiative recombination of photogenerated excitons in PyTz-COF was greatly suppressed due to its bicontinuous heterojunction.<sup>[17]</sup> Time-resolved photoluminescence (TRPL) spectroscopy revealed the PL decay kinetics (Figure 2e) as the average lifetimes excited at 320 nm were estimated to be 2.3 and 4.4 ns for PyBp- and PyTz-COFs, respectively. The extended electron delocalization on Tz-based acceptor subunits have guaranteed its elongated lifetime. Contributions were also found from crystallinity of COF because the amorphous PyTz polymer (PyTz-amp, see in Supporting Information) displayed shorter lifetime of 3.2 ns. The ordered Py and Tz array in crystalline PyTz-COF benefitted charge separation and transportation (Figure S13, Supporting Information).<sup>[18]</sup>

In the nanosecond transient time profile of hole-polarons (Figure 2f), a much stronger transient-absorption signal observed for PyTz-COF over PyBp-COF (Figure S14, Supporting Information) is also indicative of the superior charge separation ability of PyTz-COF. The fitting plot in Figure 2f revealed that the lifetime of the charge-separated state of PyTz-COF was as long as 6.93 ns.

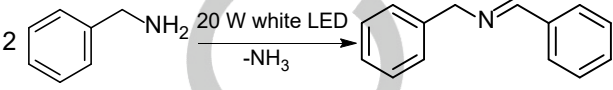
Therefore, intense signals and long lifetime discovered under steady state and transient state have demonstrated that the ordered D-A heterojunction lead to an efficient charge separation and transportation.<sup>[19,20]</sup>

**Photocatalytic Activities.** Encouraged by PyTz-COF's photoelectronic properties, we thus evaluated its photocatalytic activity using visible-light-driven coupling reaction of primary amines. Photocatalytic aerobic oxidation of primary amines to imine is an environmentally benign alternative for traditional oxidative coupling as it proceeds under mild condition. Benzylamine was used as substrate to optimize visible-light-driven coupling using PyTz-COF as the photocatalyst (Table 1). The reaction did not occur in the absence of either a catalyst or light, as expected for a photocatalytic reaction. Neither PyBp-COF nor PyTz-amp showed the catalytic efficiency comparable to that of PyTz-COF. Notably, sustained photocatalytic activity and crystallinity of PyTz-COF was evidenced after at least 5 runs of catalytic reaction. (Figure S15 and S16, Supporting Information). Moreover, various arylmethanamines were tested to evaluate the substrate scope (Table 2). It was found that arylmethanamines with larger substituents tended to have poorer conversions, which could be explained by hindered access to the pores of COF photocatalyst.

Electron paramagnetic resonance (EPR) spectroscopy was further exploited for elucidating reaction mechanism. After illuminating the reaction system for 1 min, the signal for an adduct of superoxide radical anion with 5,5-dimethyl-1-pyrroline N-oxide

(DMPO) aroused in an air saturated  $\text{CH}_3\text{CN}$  solution containing PyTz-COF and DMPO (Figure S17 and S18 in Supporting Information). With  $\text{AgNO}_3$  as an electron scavenger, coupling of benzylamine did not occur, which indicated that the photogenerated  $e^-$  in PyTz-COF reduced absorbed oxygen molecules to superoxide radical anions for the subsequent oxidation of the substrates to products.

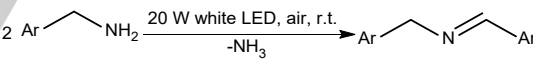
**Table 1.** Optimization of oxidative coupling of benzylamine.<sup>[a]</sup>

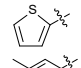
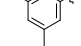


Entry	20 W white LED	Photocatalyst	air	Conversion [%] <sup>[b]</sup>
1	on	PyTz-COF	+	90
2	off	PyTz-COF	+	none
3	on	none	+	none
4	on	PyTz-COF	-	none
5	on	PyTz-amp	+	26
6	on	PyBp-COF	+	34
7 <sup>[c]</sup>	on	PyTz-COF	-	none

[a] Conditions: Benzylamine (0.6 mmol) and catalyst (0.01 mmol) in  $\text{CH}_3\text{CN}$  (2 mL) and  $\text{H}_2\text{O}$  (1 mL) for 2 h. [b] Determined by  $^1\text{H}$  NMR of the crude mixture. <sup>c</sup>Adding  $\text{AgNO}_3$  (200 mg).

**Table 2.** Photocatalytic Aerobic Oxidation of Arylmethanamines.<sup>[a]</sup>



Entry	Ar-	Time [h]	Conversion [%] <sup>[b]</sup>	Selectivity [%] <sup>[c]</sup>
1	$\text{C}_6\text{H}_5$	2	90	97
2	4-F- $\text{C}_6\text{H}_4$	4	71	100
3	4-Me- $\text{C}_6\text{H}_4$	9	67	100
4	4-OMe- $\text{C}_6\text{H}_4$	9	68	100
5	4-t-Bu- $\text{C}_6\text{H}_4$	18	50	100
6		5	100	96
7		12	77	96

[a] Conditions: Amine (0.5 mmol) and PyTz-COF (0.01 mmol) in  $\text{CH}_3\text{CN}$  (2 mL) and  $\text{H}_2\text{O}$  (1 mL). [b] Determined by  $^1\text{H}$  NMR of the crude mixture.

## RESEARCH ARTICLE

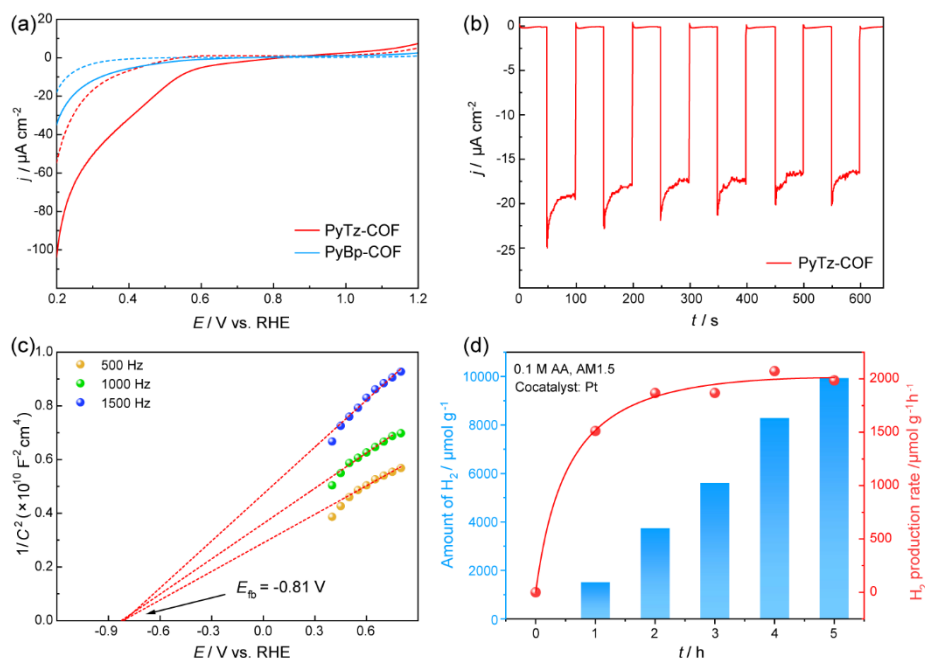


**Figure 3.** (a) LSV of PyTz-COF (red) and PyBp-COF (blue) in the dark (dashed line) and under AM1.5 light irradiation (solid line) in phosphate buffer solution. (b) Amperometric *i-t* curve of PyTz-COF under chopped light irradiation at 0.4 V vs. RHE. (c) Mott-Schottky plots of PyTz-COF at 500, 1000, and 1500 Hz. The interception at potential axis shows the flat-band potential of -0.81 V vs. RHE. (d) Time-dependent photocatalytic hydrogen production (amount and rate) of PyTz-COF under AM1.5 light irradiation (468 mW cm<sup>-2</sup>) for 5 h.

**Photoelectrochemical Properties.** The exceptional photoelectronic properties of the crystalline PyTz-COF prompted us for further evaluation of its electrochemical properties. Under AM 1.5 light illumination, cathodic photocurrent of PyTz-COF exhibited a current up to 100  $\mu\text{A cm}^{-2}$  at 0.2 V vs. RHE according to its linear sweep voltammograms (LSV) in a phosphate buffered electrolyte (pH 7.0) (Figure 3a). This value ranks the highest among all the reported COF photocathodes including imine-linked COF (BDT-ETTA)<sup>14c</sup> ( $\sim 2.5 \mu\text{A cm}^{-2}$ ) and g-C<sub>18</sub>N<sub>3</sub>-COF<sup>[20]</sup> ( $\sim 45 \mu\text{A cm}^{-2}$ ). At 0.4 V vs. RHE, photocurrent response of PyTz-COF ( $\sim 17.5 \mu\text{A cm}^{-2}$ ) (Figure 3b) was nearly 3-fold higher than that of PyBp-COF ( $\sim 5.7 \mu\text{A cm}^{-2}$ ) estimated from Figure 3a. The semicircle with much smaller diameter in the Nyquist plot of PyTz-COF further revealed its faster interfacial charge transfer (Figure S19, Supporting Information).<sup>[21]</sup> Additionally, the positive slopes of the Mott-Schottky plots in Figure 3c suggested that PyTz-COF is an *n*-type semiconductor.<sup>[22]</sup> With the calculated flat-band potential of -0.81 V vs. RHE, PyTz-COF is expected to be able to drive proton reduction as its CBM potential is more negative than water reduction potential (0 V vs. RHE).<sup>[23]</sup>

We then evaluated the photocatalytic hydrogen evolution performance of PyTz-COF under simulated sunlight (AM 1.5). In a typical process, PyTz-COF powder (35 mg) was added to aqueous ascorbic acid (0.1 M) solution containing 27  $\mu\text{L}$  hexachloroplatinic acid solution (8 wt%,  $\sim 3 \text{ wt}\%$  Pt basis) where ascorbic acid was used as sacrificial electron donor. The amount of hydrogen evolved from the system increased rapidly during the first hour and then moderately in the second hour (Figure 3d). In the fourth hour, the hydrogen evolution rate (HER) could reach its peak value of 2072.4  $\mu\text{mol g}^{-1} \text{h}^{-1}$  which exceeds the values of many previously reported COFs, such as COF TpTz-COF<sup>[11c]</sup> (941  $\mu\text{mol g}^{-1} \text{h}^{-1}$ ), g-C<sub>18</sub>N<sub>3</sub>-COF<sup>[22]</sup> (292  $\mu\text{mol g}^{-1} \text{h}^{-1}$ ), BtCOF-150<sup>[24]</sup> (750  $\mu\text{mol g}^{-1} \text{h}^{-1}$ ), N<sub>2</sub>-COF with molecular cobalt complexes<sup>[25]</sup>

(782  $\mu\text{mol g}^{-1} \text{h}^{-1}$ ), and NTU-BDA-THTA<sup>[26]</sup> (1172  $\mu\text{mol g}^{-1} \text{h}^{-1}$ ). Comprehensive comparisons of HER performance among the reported COFs can be found in Table S2 in Supporting Information. Photocatalytic experiments under identical condition using monomer TzDA or PyTA as photocatalysts displayed far lower or trace amount of hydrogen generation (Figure S20, Supporting Information), highlighting the role of reticular chemistry in the construction of photocatalytically active materials. Notably, it was found that Pt loading weight was actually crucial to the hydrogen production rate: Higher production rate with lower Pt content (Figure S21, Supporting Information). The cyclic catalytic performance for water splitting was examined by running the experiment for consecutive five cycles (4 h for each cycle) (Figure S22, Supporting Information). Actually, the amount of hydrogen has been increasing in the first three cycles, and then started to decrease in the fourth cycle. It still maintained at a production rate over 1000  $\mu\text{mol g}^{-1} \text{h}^{-1}$  even in the last two cycles. The crystallinity of PyTz-COF after the fifth cycle is moderately decreased as revealed by PXRD analysis (Figure S23, Supporting Information).

## Conclusion

In summary, we have constructed PyTz-COF that bears finely organized D-A heterojunction formed from columnar stacking of Py and Tz building blocks, which enabled effective photogenerated charge separation and efficient charge migration. It displayed visible light-driven photocatalytic activity in oxygen reduction to superoxide radical and subsequent coupling of (arylmethyl)amines. PyTz-COF's photocurrent response could reach as high as 100  $\mu\text{A cm}^{-2}$ , and the sunlight-driven hydrogen production water splitting photoelectrochemically catalyzed by

## RESEARCH ARTICLE

PyTz-COF could be reached at a rate up to 2072.4  $\mu\text{mol g}^{-1} \text{h}^{-1}$ . The described work would inspire future development of sunlight-driven photocatalysts.

## Conflicts of interest

There are no conflicts to declare.

## Acknowledgements

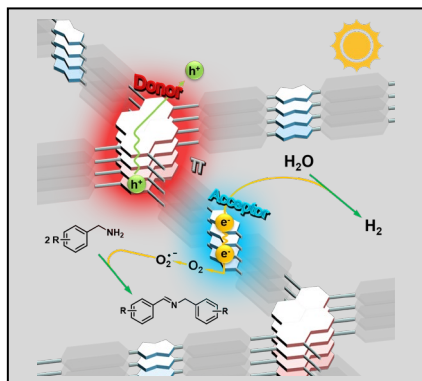
This work is supported by the National Key Research and Development Program of China (2017YFA0206500), the National Natural Science Foundation of China (No. 21522105, 21871281, and 51861145313), and the Science & Technology Commission of Shanghai Municipality (17JC1404000). We thank the scientific and technical support from ShanghaiTech-SARI Joint Laboratory of Low-Carbon Energy Science and Analytical Instrumentation Center (Contract no. SPST-AIC10112914), SPST, ShanghaiTech University. The authors thank Prof. Zhi Liu at ShanghaiTech University for beneficial discussion and scientific support, and Dr. Yajun Zhang at Lanzhou Institute of Chemical Physics, CAS, for help in transient absorption spectroscopy.

**Keywords:** donor-acceptor • charge transfer • covalent organic frameworks • solar energy harvesting • hydrogen production

- [1] A. Fujishima, K. Honda, *Nature* **1972**, 238, 37.
- [2] A. M. Smith, S. Nie, *Acc. Chem. Res.* **2010**, 43, 190.
- [3] F. E. Osterloh, *Chem. Soc. Rev.* **2013**, 42, 2294.
- [4] a) S. Bai, N. Zhang, C. Gao, Y. Xiong, *Nano Energy* **2018**, 53, 296; b) C. G. Silva, I. Luz, F. X. L. I. Xamena, A. Corma, H. Garcia, *Chem. -Eur. J.* **2010**, 16, 11133.
- [5] C. S. Diercks, Y. Liu, K. E. Cordova, O. M. Yaghi, *Nat. Mater.* **2018**, 17, 301.
- [6] a) C. S. Diercks, O. M. Yaghi, *Science* **2017**, 355, 923; b) Côté, P. Adrien, Benin, I. Annabelle, Ockwig, W. Nathan, O'Keefe, Michael, Matzger, J. Adam, *Science* **2005**, 310, 1166; c) S. Ding, W. Wang, *Chem. Soc. Rev.* **2013**, 42, 548; d) N. Huang, P. Wang, D. Jiang, *Nat. Rev. Mater.* **2016**, 1, 16068; e) S. Kandambeth, K. Dey, R. Banerjee, *J. Am. Chem. Soc.* **2019**, 141, 1807.
- [7] a) C. J. Doonan, D. J. Tranchemontagne, T. G. Glover, J. R. Hunt, O. M. Yaghi, *Nat. Chem.* **2010**, 2, 235; b) S. Lin, C. S. Diercks, Y. Zhang, N. Kornienko, E. M. Nichols, Y. Zhao, A. R. Paris, D. Kim, P. Yang, O. M. Yaghi, *Science* **2015**, 349, 1208; c) L. Ascherl, T. Sick, J. T. Margraf, S. H. Lapidus, M. Calik, C. Hettstedt, K. Karaghiosoff, M. Doblinger, T. Clark, K. W. Chapman, *Nat. Chem.* **2016**, 8, 310; d) E. Jin, M. Asada, Q. Xu, S. Dalapati, M. Addicoat, M. A. Brady, H. Xu, T. Nakamura, T. Heine, Q. Chen, *Science* **2017**, 357, 673; e) S. Wang, Q. Wang, P. Shao, Y. Han, X. Gao, L. Ma, S. Yuan, X. Ma, J. Zhou, X. Feng, *J. Am. Chem. Soc.* **2017**, 139, 4258; f) K. Dey, M. Pal, K. C. Rout, S. K. H. A. Das, R. Mukherjee, U. K. Kharul, R. Banerjee, *J. Am. Chem. Soc.* **2017**, 139, 13083.
- [8] a) L. Guo, Y. Niu, H. Xu, Q. Li, S. Razzaque, Q. Huang, S. Jin, B. Tan, *J. Mater. Chem.* **2018**, 6, 19775; b) S. Jin, X. Ding, X. Feng, M. Supur, K. Furukawa, S. Takahashi, M. Addicoat, M. E. Elkhoully, T. Nakamura, S. Irie, *Angew. Chem. Int. Ed.* **2013**, 52, 2017; c) M. Calik, F. Auras, L. M. Salonen, K. Bader, I. Grill, M. Handloser, D. D. Medina, M. Dogru, F. Lobermann, D. Trauner, *J. Am. Chem. Soc.* **2014**, 136, 17802.
- [9] a) D. Bevk, L. Marin, L. Lutsen, D. Vanderzande, W. Maes, *RSC Adv.* **2013**, 3, 11418; b) S. Van Mierloo, A. Hadipour, M.-J. Spijkman, N. Van den Brande, B. Ruttens, J. Kesters, J. D'Haen, G. Van Assche, D. M. de Leeuw, T. Aernouts, J. Manca, L. Lutsen, D. J. Vanderzande, W. Maes, *Chem. Mater.* **2012**, 24, 587; c) M. Samal, S. Valligatta, N. A. Saad, M. V. Rao, D. N. Rao, R. Sahu, B. P. Biswal, *Chem. Commun.* **2019**, 55, 11025.
- [10] B. P. Biswal, H. A. Vignolo-Gonzalez, T. Banerjee, L. Grunenberg, G. Savasci, K. Gottschling, J. Nuss, C. Ochsenfeld, B. V. Lotsch, *J. Am. Chem. Soc.* **2019**, 141, 11082.
- [11] R. S. Sprick, J. Jiang, B. Bonillo, S. Ren, T. Ratvijitvech, P. Guiglion, M. A. Zwijnenburg, D. J. Adams, A. I. Cooper, *J. Am. Chem. Soc.* **2015**, 137, 3265.
- [12] a) F. Auras, L. Ascherl, A. H. Hakimioun, J. T. Margraf, F. C. Hanusch, S. Reuter, D. Bessinger, M. Doblinger, C. Hettstedt, K. Karaghiosoff, *J. Am. Chem. Soc.* **2016**, 138, 16703; b) L. Wang, C. Zeng, H. Xu, P. Yin, D. Chen, J. Deng, M. Li, N. Zheng, C. Gu, Y. Ma, *Chem. Sci.* **2019**, 10, 1023; c) Y. Li, Q. Chen, T. Xu, Z. Xie, J. Liu, X. Yu, S. Ma, T. Qin, L. Chen, *J. Am. Chem. Soc.* **2019**, 141, 13822; d) T. Banerjee, F. Haase, S. Trenker, B. P. Biswal, G. Savasci, V. Duppel, I. L. Moudrakovski, C. Ochsenfeld, B. V. Lotsch, *Nat. Commun.* **2019**, 10, 1.
- [13] a) P. F. Wei, M. Z. Qi, Z. P. Wang, S. Y. Ding, W. Yu, Q. Liu, L. K. Wang, H. Z. Wang, W. K. An, W. Wang, *J. Am. Chem. Soc.* **2018**, 140, 4623; b) W. Liu, Q. Su, P. Ju, B. Guo, H. Zhou, G. Li, Q. Wu, *ChemSusChem* **2017**, 10, 664.
- [14] a) L. Stegbauer, K. Schwinghammer, B. V. Lotsch, *Chem. Sci.* **2014**, 5, 2789; b) X. Wang, L. Chen, S. Y. Chong, M. A. Little, Y. Wu, W. Zhu, R. Clowes, Y. Yan, M. A. Zwijnenburg, R. S. Sprick, A. I. Cooper, *Nat. Chem.* **2018**, 10, 1180; c) T. Sick, A. G. Hufnagel, J. Kampmann, I. Kondofersky, M. Calik, J. M. Rotter, A. M. Evans, M. Doblinger, S. A. Herbert, K. Peters, *J. Am. Chem. Soc.* **2017**, 140, 2085; d) S. Bi, C. Yang, W. Zhang, J. Xu, L. Liu, D. Wu, X. Wang, Y. Han, Q. Liang, F. Zhang, *Nat. Commun.* **2019**, 10, 2467; e) W. Chen, L. Wang, D. Mo, F. He, Z. Wen, X. Wu, H. Xu, L. Chen, *Angew. Chem. Int. Ed.* **2020**, 59, 16902.
- [15] a) K. Lei, D. Wang, L. Ye, M. Kou, Y. Deng, Z. Ma, L. Wang, Y. Kong, *ChemSusChem* **2020**, 13, 1725; b) Y. Chen, B. Wang, S. Lin, Y. Zhang, X. Wang, *J. Phys. Chem. C* **2014**, 118, 29981.
- [16] a) S. Ghosh, N. A. Kouame, L. Ramos, S. Remita, A. Dazzi, A. Deniset-Besseau, P. Beauvier, F. Goubard, P. Aubert, H. Remita, *Nat. Mater.* **2015**, 14, 505; b) Y. Xu, M. A. A. Schoonen, *Am. Mineral.* **2000**, 85, 543.
- [17] a) L. Jiang, X. Yuan, G. Zeng, Z. Wu, J. Liang, X. Chen, L. Leng, H. Wang, H. Wang, *Appl. Catal., B* **2018**, 221, 715; b) H. She, H. Zhou, L. Li, L. Wang, J. Huang, Q. Wang, *ACS Sustainable Chem. Eng.* **2018**, 6, 11939; c) C. Ye, J. Li, Z. Li, X. Li, X. Fan, L. Zhang, B. Chen, C. Tung, L. Wu, *ACS Catal.* **2015**, 5, 6973.
- [18] a) X. Ding, L. Chen, Y. Honsho, X. Feng, O. Saengsawang, J. Guo, A. Saeki, S. Seki, S. Irie, S. Nagase, *J. Am. Chem. Soc.* **2011**, 133, 14510; b) E. L. Spittler, W. R. Dichtel, *Nat. Chem.* **2010**, 2, 672; c) X. Ding, X. Feng, A. Saeki, S. Seki, A. Nagai, D. Jiang, *Chem. Commun.* **2012**, 48, 8952.
- [19] a) M. A. Ruderer, S. Guo, R. Meier, H. Chiang, V. Korstgens, J. Wiedersich, J. Perlich, S. V. Roth, P. Mullerbuschbaum, *Adv. Funct. Mater.* **2011**, 21, 3382; b) J. Peet, J. Y. Kim, N. E. Coates, W. Ma, D. Moses, A. J. Heeger, G. C. Bazan, *Nat. Mater.* **2007**, 6, 497; c) D. D. Medina, V. Werner, F. Auras, R. Tautz, M. Dogru, J. Schuster, S. Linke, M. Doblinger, J. Feldmann, P. Knochel, *ACS Nano* **2014**, 8, 4042.
- [20] S. Wei, F. Zhang, W. Zhang, P. Qiang, K. Yu, X. Fu, D. Wu, S. Bi, *J. Am. Chem. Soc.* **2019**, 141, 14272.
- [21] V. Spagnol, E. M. M. Sutter, C. Debiemchouvy, H. Cachet, B. Baroux, *Electrochim. Acta* **2009**, 54, 1228.
- [22] J. Zhang, X. Chen, K. Takanabe, K. Maeda, K. Domen, J. D. Epping, X. Fu, M. Antonietti, X. Wang, *Angew. Chem. Int. Ed.* **2010**, 49, 441.
- [23] L. F. Schneemeyer, M. S. Wrighton, *J. Am. Chem. Soc.* **1979**, 101, 6496.
- [24] S. Ghosh, A. Nakada, M. Springer, T. Kawaguchi, S. Seki, *J. Am. Chem. Soc.* **2020**, 142, 9752.
- [25] T. Banerjee, F. Haase, G. Savasci, K. Gottschling, C. Ochsenfeld, B. V. Lotsch, *J. Am. Chem. Soc.* **2017**, 139, 16228.
- [26] H. Wang, C. Qian, J. Liu, Y. Zeng, Y. Zhao, *J. Am. Chem. Soc.* **2020**, 142, 4862.

## RESEARCH ARTICLE

## Entry for the Table of Contents



Covalent organic frameworks constructed from electron-rich pyrene and electron deficient thiazolo[5,4-d]thiazole bears donor-acceptor features. It creates efficient carrier pathways for efficient separation of photogenerated holes and electrons. The COF thus demonstrated high photocatalytic activity for amine-coupling reactions and hydrogen production for water splitting.